JOC The Journal of Organic Chemistry

pubs.acs.org/joc Article

Activation of O-Electrophiles *via* Structural and Solvent Effects: S_N2@O Reaction of Cyclic Diacyl Peroxides with Enol Acetates

Vera A. Vil', Evgenii S. Gorlov, Diana V. Shuingalieva, Artem Yu. Kunitsyn, Nikolai V. Krivoshchapov, Michael G. Medvedev, Igor V. Alabugin,* and Alexander O. Terent'ev*

Cite This: *J. Org. Chem.* 2022, 87, 13980–13989 Read Online

ACCESS | Metrics & More | Article Recommendations | Supporting Information

ABSTRACT: The reactions of O-electrophiles, such as organic peroxides, with carbon nucleophiles are an umpolung alternative to the common approaches to C–O bond formation. Nucleophilic substitution at the oxygen atom of cyclic diacyl peroxides by enol acetates with the following deacylation leads to α-acyloxyketones with an appended carboxylic acid in 28–87% yields. The effect of fluorinated alcohols on the oxidative functionalization of enol acetates by cyclic diacyl peroxides was studied experimentally and computationally. Computational analysis reveals that the key step proceeds as a direct substitution nucleophilic bimolecular (S_N2) reaction at oxygen (S_N2@O). CF_3CH_2OH has a dual role in assisting in both steps of the reaction cascade: it lowers the energy of the S_N2@O activation step by hydrogen bonding to a remote carbonyl and promotes the deacylation of the cationic intermediate.

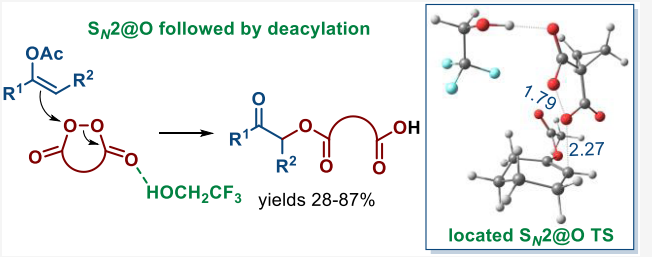

INTRODUCTION

Nucleophilic substitution is a fundamental organic textbook transformation.[1,2] Generally, nucleophilic substitution involves the replacement of a good leaving group at an electron-deficient carbon atom. Hence, nucleophilic substitution at the carbon electrophilic center by the oxygen nucleophile is the ubiquitous strategy for making the C–O bonds (Scheme 1). Nucleophilic substitutions at phosphorus,[3] sulfur,[4] and silicon[5] atoms have also found synthetic applications.

In contrast, nucleophilic substitution at an oxygen atom is far less common (Scheme 1a) because O–X bonds are usually unfavorably polarized and because electron-rich oxygen atoms are poor targets for nucleophiles. As a result, the "umpolung" approaches where a carbon-centered nucleophile reacts with an oxygen electrophile are relatively scarce.

Organic peroxides with the electron-withdrawing groups could address this limitation and serve as a potentially useful family of "OR" electrophiles. Indeed, scattered successes with acyclic diacyl peroxides,[6−12] *tert*-butyl perbenzoate,[13] peroxydicarbonates,[14] sulfonyl peroxides,[15−17] and bis(trimethylsilyl) peroxide[18] (Scheme 1b) indicate that, although these reactions are considerably less established than their carbon-based counterparts, the electrophilic alkoxyl ("RO^+") transfer can offer an alternative to traditional methods for the C–O bond formation.[19] In this work, we expand the scope of such processes for oxidative functionalization of enol acetates. We show that cyclic diacyl peroxides react as O-electrophiles with these nucleophilic substrates with the formation of α-acyloxyketones with a pendant carboxylic acid (Scheme 1c).

Scheme 1. Overview of RO-Functionalization Strategies

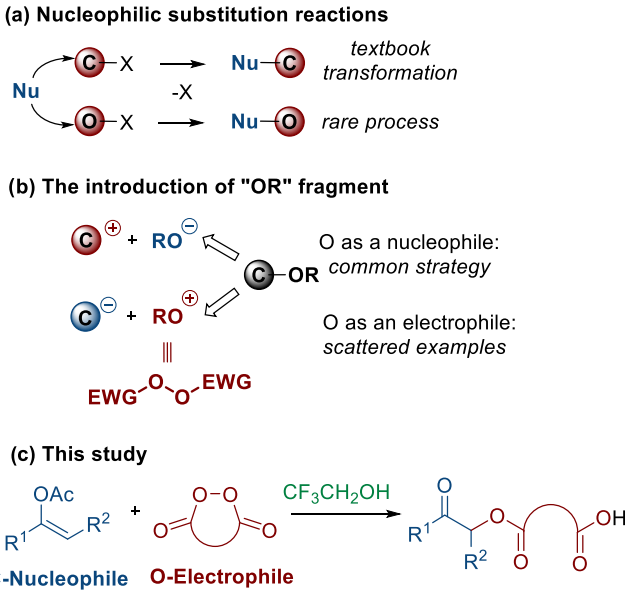

Received: July 12, 2022
Published: October 12, 2022

In the last decade, cyclic diacyl peroxides,[20] first prepared in the 1950s,[21−25] became versatile O-electrophilic reagents for the introduction of oxygen functionalities into arenes,[26−29] alkenes,[30−32] heterocycles,[33] dicarbonyl compounds,[34,35] and their derivatives[36,37] (Scheme 2). Cyclic diacyl peroxides are more reactive than acyclic diacyl peroxides[38−40] mostly because the anomeric $n_O \rightarrow \sigma^*_{CO}$ interactions in cyclic diacyl peroxides are considerably weaker in comparison to the analogous acyclic peroxides (Scheme 2a,b).[41] These differences in reactivity can be further amplified by a more favorable antiperiplanar arrangement of the breaking O−O bond to the σ^*CO bond of the carbonyl in the substitution nucleophilic bimolecular (S_N2) process. As the negative charge accumulates at the departing oxygen of the O−O bond in the transition state (TS), such anomeric interaction grows stronger and provides selective TS stabilization (Scheme 2b).[41] A similar pattern of anomeric assistance, albeit with an sp^3 σ^*_{C-O}, was used to control the regioselectivity of nucleophilic attack at an O−O bond by Dussault (Scheme 2c).[42]

In addition to organic peroxides[6,8−10,14] and transition-metal peroxides,[43−45] other oxygen electrophiles have been used for the α-oxidation of carbonyl compounds. In particular, oxaziridines, including *N*-sulfonyloxaziridines,[46−48] were devised for the asymmetric oxidation of enolate substrates to optically active α-hydroxy carbonyl compounds.[49−55] The geometry of the transition state for the oxidation by *N*-sulfonyloxaziridines was established as planar.[46,56]

This work focuses on the mechanism and structure of transition states for the interaction of cyclic diacyl peroxides as O-electrophiles with carbon nucleophiles, enol acetates. In addition, we were intrigued by the role of fluorinated alcohol solvents in the reactions of cyclic diacyl peroxides.[27,29,57−60] These solvents have recently been recognized as remarkable media for a variety of chemical transformations due to their strong hydrogen-bonding ability and high polarity.[61,62] In the present work, we illustrate how CF_3CH_2OH is directly involved in the transition state of the nucleophilic substitution step to assist in the acetyl group elimination (Scheme 2c).

Scheme 2. Comparison of Acyclic Peroxides (a) and Cyclic Diacyl Peroxides (b) as O-Electrophiles. (c) Stereoelectronic Patterns for TS Stabilization in Reactions of Peroxides with Nucleophiles

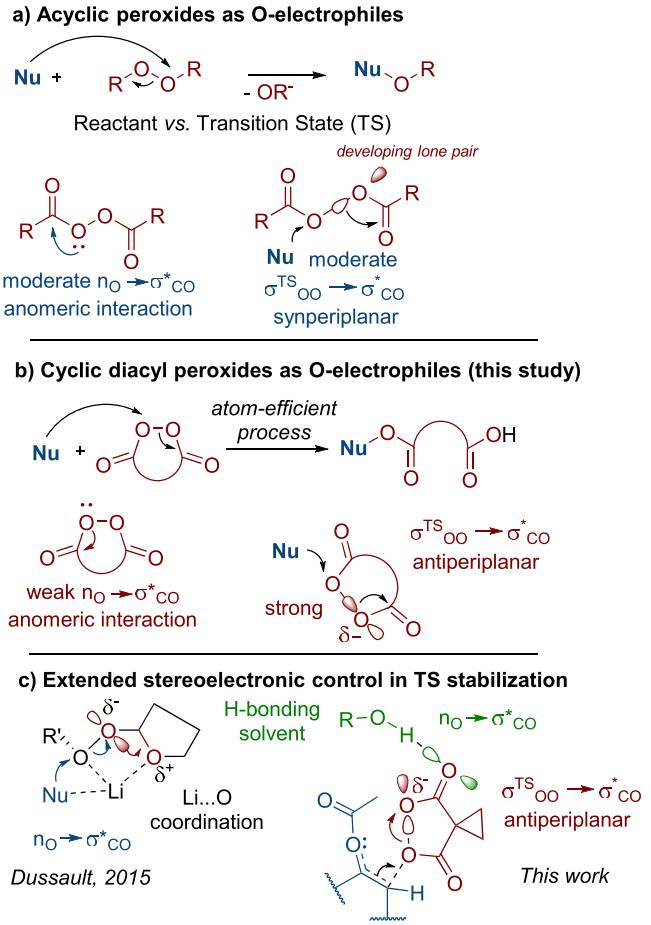

RESULTS AND DISCUSSION

To gain better insight into the oxidative functionalization of enol acetates by cyclic diacyl peroxides, we investigated the reaction of cyclohept-1-*en*-1-yl acetate **1a** using cyclopropyl malonoyl peroxide **2** as a model O-electrophile (Table 1).

Initially, the reaction of enol acetate **1a** with cyclic diacyl peroxide **2** was tested in CH_2Cl_2 and tetrahydrofuran (THF) at 20−25 °C for 24 h (Table 1, entries 1 and 2). These solvents worked well in our previous studies,[36] but no conversion of **1a** was observed in this case. The addition of *p*-TsOH·H_2O (entry 3) led to a low (28%) yield of **3a**. Increasing the reaction temperature in THF did not improve the yield of **3a** (entry 4), possibly due to the cleavage of THF in the presence of the electrophile and *p*-TsOH·H_2O.[63−65] The 33% yield of **3a** was obtained in the case of CH_3CN as the solvent (entry 5). However, the yield of **3a** increased after switching from catalytic amounts of acid to acidic solvents such as acetic acid and trifluoroethanol (entries 6 and 7). Fluorinated alcohols were previously shown to be effective media for oxidative coupling using cyclic diacyl peroxides.[33] Hexafluoroisopropanol was apparently too acidic, resulting in the yield of product **3a** dropping to 36% with the concomitant formation of a glassy mass insoluble in organic solvents (entry 8). The highest yields of product **3a** were observed in refluxing CF_3CH_2OH for 3 h (Table 1, entry 9). Purification using column chromatography on SiO_2 (method A) resulted in a 57% isolated yield of the α-acyloxylated ketone **3a** (entry 9, Table 1 footnote d). Isolation of the pure product **3a** *via* carboxylate formation with subsequent acidification afforded 68% of the α-acyloxylated ketone **3a** after isolation (entry 9, Table 1 footnote e). The use of 2 equiv of peroxide **2a** did not result in a better **3a** yield (entry 10). The main byproduct in entries 3−7 was cycloheptanone as a result of **1a** hydrolysis.

With the optimized conditions in hand (Table 1, entry 9), we next explored the substrate scope by testing the utility of oxidative functionalization of enol acetates **1** by cyclic diacyl peroxides **2**, **4**, and **6** for the syntheses of the α-acyloxylated ketones **3**, **5**, and **7** (Scheme 3).

Aliphatic enol acetates **1a−d** and enol acetates from aryl ketones **1e−k** were compatible with the reaction conditions, giving the corresponding products **3a−d** and **3e−k** in 49−68 and 52−87% yields, respectively. The product **3l** with two benzylic groups was synthesized in 50% yield. Application of various cyclic diacyl peroxides, such as cyclopropyl malonoyl peroxide **2**, cyclobutyl malonoyl peroxide **4**, and phthaloyl peroxide **6**, resulted in α-acyloxylated ketones **3k**, **5k**, and **7k**, respectively, in good yields (Scheme 3). The main side products were the corresponding ketones, which do not react with the peroxide. It is worth noting that the reaction with the

https://doi.org/10.1021/acs.joc.2c01634
J. Org. Chem. 2022, 87, 13980−13989

Table 1. Optimization of the Reaction of Enol Acetate 1a with Peroxide 2[a]

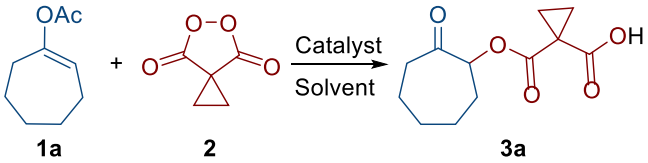

1a 2 3a

entry	solvent	temp. (°C)	catalyst	time (h)	convn 1a (%)[b]	yield 3a (%)[b]
1	CH_2Cl_2	20–25		24	n.r.	
2	THF	20–25		24	n.r.	
3	THF	20–25	*p*-TsOH·H_2O	24	76	28
4	THF	reflux (≈66 °C)	*p*-TsOH·H_2O	3	19	17
5	CH_3CN	reflux (≈82 °C)	*p*-TsOH·H_2O	3	81	33
6	AcOH	reflux (≈119 °C)		3	>95	49
7	CF_3CH_2OH	20–25		24	81	52
8	$(CF_3)_2CHOH$	20–25		24	>95	36[c]
9	CF_3CH_2OH	reflux (≈78 °C)		3	>95	70 (57[d], 68[e])
10[f]	CF_3CH_2OH	reflux (≈78 °C)		3	>95	58

[a]General conditions: the mixture of cyclopropyl malonoyl peroxide **2** (1.1 mmol, 140.9 mg) with enol acetate **1a** (1.0 mmol, 154.2 mg) and catalyst (0.02 mmol) in solvent (2 mL) was stirred at the certain temperature for 3–24 h. [b]On ^{1}H NMR. [c]Formation of a glassy mass insoluble in organic solvents. [d]Isolated yield of **3a** after column chromatography (method A, see the Supporting Information for details). [e]Isolated yield of **3a** after carboxylate formation with the following acidification (method B, see SI for details). [f]Peroxide **2** (2 mmol) was used.

oxidation-sensitive acetyl furan **1m** resulted in a mixture of inseparable products. The enol acetate **1n** prepared from dicarbonyl compound did not react under our reaction conditions. To our delight, the reaction was compatible with enol acetate **1o** synthesized from aldehyde to give a moderate (45%) yield of product **3o**. Unsaturated enol acetate **1p** was transformed into acyloxy product **3p** in 28% yield. The side product of C–C coupling **3p′** was isolated in 31% yield (Scheme 3).

Next, we focused on the mechanism of this new reaction and the impact of the fluorinated alcohol on cyclic diacyl peroxide reactivity.

Cyclic voltammetry (CV) was used to evaluate the reduction potentials of peroxide **2** in CH_3CN and CF_3CH_2OH (Figure 1). The solvents remained unreactive in the cathodic reduction under the potential up to −2.5 V (Figure 1, curves a and c). The CV experiments showed the oxidation peaks of cyclopropyl malonoyl peroxide **2** at 1.6 V (Figure 1, curves b and d). Based on the studies of electrochemical peroxide reduction,[66−70] cyclopropyl malonoyl peroxide **2** first probably produced the distonic radical-anion intermediate with an unpaired electron on one oxygen atom and a negative charge on the other *via* dissociative electron transfer (DET). The resulting radical anion could be reduced to a dianion before diffusion from the electrode and then protonated in the reaction media. Alternatively, the radical anion could be protonated by the reaction media, in particular by the acidic TFE, to produce a carboxyl radical. If decarboxylation of the carboxyl radical can be avoided,[71,72] it could be further reduced and subsequently protonated to result in the corresponding malonic acid.[73] In the presence of acidic TFE (Figure 1, curves b and d), the reduction **2** peak became higher and broader, possibly indicating the influence of TFE on the mass or electron transfer rates, probably due to hydrogen bonding.

Considering the possibility of nucleophilic substitution at oxygen (S_N2@O) in a similar reaction, demonstrated by Tomkinson and co-workers,[74] we proposed a two-stage mechanism for our reaction with the nucleophilic attack of enol ether **1** at the oxygen atom of peroxide **2** in the first step and elimination of the acyl group originating from **1** in the second step. To understand this mechanism at the atomic level and to elucidate the key factors controlling the pathway, we have carried out a computational study.

All quantum chemical calculations were performed with Gaussian16 A.03 program package at PBE0[75]-D3BJ[76]/6-311++G(d,p)[77−81]/CPCM(CF_3CH_2OH)[82] level of theory. PBE0 functional is known to provide accurate results for organic reactions and has been shown to be well-grounded in theory.[83−85] Harmonic frequencies were computed for all located stationary points to ensure their types and calculate quasi-harmonically[86] corrected free energies with GoodVibes[87] (temperature 351 K, concentration 1 mol L^{-1}). Conformational searches with CREST[88] were performed for **IM1** and **IM2** (Schemes 4 and 5). Transition state (TS) searches were run from geometries preoptimized at the same level of theory with forming and breaking bonds constrained at 2.0 Å following the approach previously developed by some of us.[89]

As shown by the Tomkinson group,[74] cyclic diacyl peroxides are prone to S_N2-like nucleophilic reactions, with the O–O bond acting as an electrophile (S_N2@O) instead of the addition to the carbonyl group, the usual pathway for nucleophilic reactions at the carbonyl-containing compounds. Thus, we expect the reaction to start with the S_N2@O attack of the $\pi_{C=C}$ orbital of the enol acetate **1b** at cyclopropyl malonoyl peroxide **2**, resulting in a cyclic acetal **IM1** (Scheme 4). Note that this intermediate has two new C–O bonds connecting fragments **1b** and **2**: the first one is formed during the S_N2@O process, and the second (between cationic carbon and carbonyl group) is formed barrierlessly to stabilize the positive charge. To confirm that the proposed pathway is plausible, its S_N2@O transition state **TS1** was located with the activation free energy of 25.4 kcal mol^{-1}, which is sufficiently low for a reaction proceeding at room temperature (entry 7 in Table 1). The nucleophilic attack trajectory deviates from linearity (the C–O–O angle is 150°) due to steric hindrance from the peroxide's carbonyl group. These observations are close to Yamamoto's findings that steric factors can affect preferred trajectories for reactions between functional groups.[90] Moreover, the C–O bond formed is much longer than the breaking O–O bond, indicating that S_N2@O

https://doi.org/10.1021/acs.joc.2c01634
J. Org. Chem. 2022, 87, 13980−13989

Scheme 3. Synthesis of α-Acyloxylated Ketones 3, 5, and 7 from Enol Acetates 1

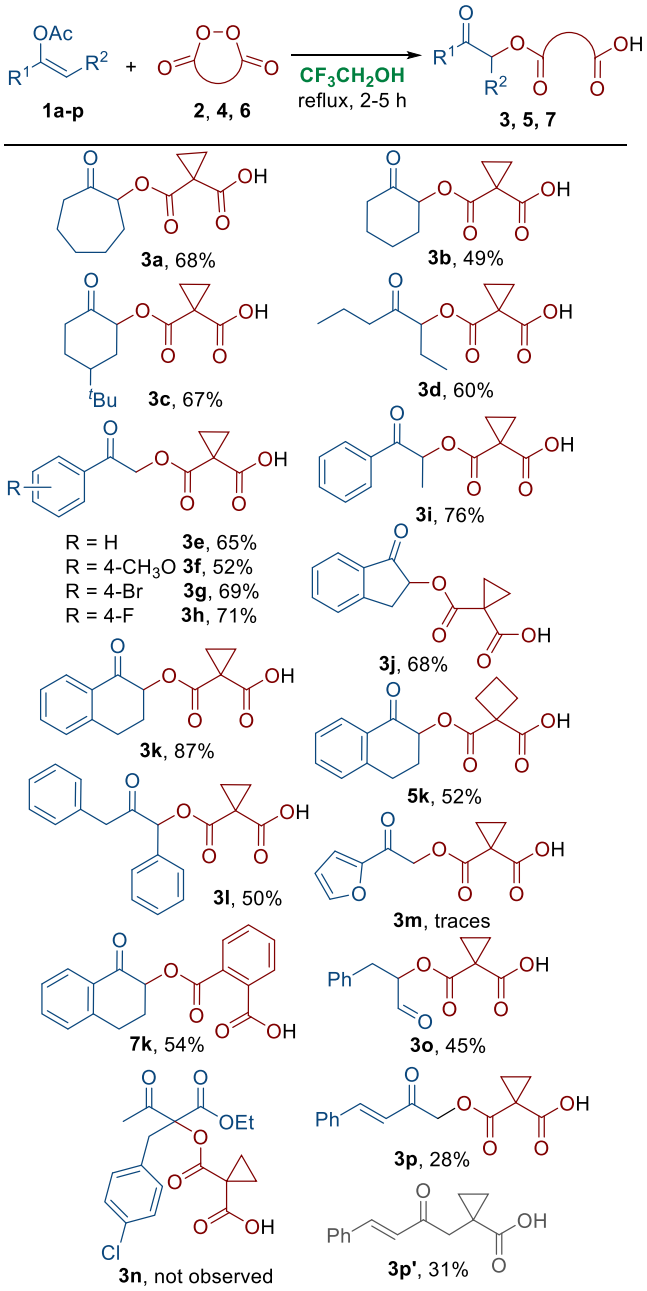

proceeds through an early TS (see inset in Scheme 4). Notably, the proposed S_N2@O process was shown to be kinetically and thermodynamically preferable over the attack at the π^*_{CO}, *i.e.*, the common path for the reactions of carbonyl compounds with nucleophiles (see Figure S5). Also, we considered a route *via* (2 + 2)-cycloaddition of **1b** and **2** but were unable to locate the corresponding TS; this path is most likely forbidden due to the interacting orbital symmetries (Scheme 4).

Interestingly, the activation energy for the S_N2@O step is lowered upon transition from vacuum (ε = 1, ΔG_a = 27.0) to implicit solvent: CF_3CH_2OH (ε = 25.4,[91] ΔG_a = 25.4) or CH_3CN (ε = 35.8,[92] ΔG_a = 25.4). This behavior indicates that the cost of charge separation is mitigated by electrostatic interactions with the solvent. Moreover, the inclusion of one explicit TFE molecule coordinated with the carbonyl group reveals an interesting effect. The solvent molecule forms a C═O···H hydrogen bond located outside of the carbonyl plane (the O−C═O···H dihedral angle ∼32°). Such a preference is different from the known H-bond preferences for the carbonyl compounds where H-bond donors coordinate with the in-plane lone pairs of oxygen.[93] This stereoelectronic preference is reminiscent of the "oxyanion hole" stabilization in enzyme active sites where the coordination of H-bond donors at the carbonyl π-bond is preferably coordinated with the oxygen lone pair. This arrangement avoids unproductive reactant stabilization and instead positions the H-bond donor on top of the new, out-of-plane oxygen lone pair that is developed from the carbonyl π-bond in the TS (the oxyanion lone pair). Such catalytic sites can provide selective and significant stabilization to the TS.[94] In our system, the inclusion of one explicit TFE molecule coordinated with the carbonyl group further lowers the S_N2@O reaction barrier by 1.5 kcal mol^{-1} (Scheme 4). Thus, explicit hydrogen bonding provides stabilization to the developing negative charge on the leaving carboxyl group and makes the complex of **2** with TFE molecule more reactive in the S_N2@O process.

^{13}C NMR spectroscopy was used to experimentally verify the hydrogen-bonding interactions of CF_3CH_2OH with the peroxyacyl groups of peroxide **2**.[57,95] Indeed when a solution of peroxide **2** in $CDCl_3$ was titrated with CF_3CH_2OH, the peroxyacyl resonance in the ^{13}C NMR spectrum was observed to shift downfield (Figure 2). These results suggest that an intermolecular hydrogen-bonding interaction between the fluorinated alcohol and the cyclic diacyl peroxide reduces the electron density of the peroxide fragment and increases its reactivity toward nucleophiles. To assess how these interactions affect the S_N2@O barrier, we investigated a transition state **TS1*TFE** having an extra hydrogen bond with an explicit CF_3CH_2OH molecule and a transition state **TS1** without such an interaction (Scheme 4). In the case of **TS1*TFE**, the activation free energy turned out to be 1.5 kcal mol^{-1} lower (Scheme 4), showing that hydrogen bonding accelerated this step.

Now let us consider the final stage of the reaction, which is the elimination of the acetyl group originating from **1b**. Based on experimental and computational results for the enol ethers,[36] the intermediate **IM1** can be expected to rearrange into mixed anhydride **IM3**, which converts into the final product **3b** *via* the elimination of the acetyl group (Scheme 5). To check if this route is energetically feasible, we located a TS of **IM2** → **3b** transformation. However, this step has a surprisingly high activation free energy of 40.6 kcal mol^{-1} (**TS3**). The height of this barrier suggests that **IM2** constitutes a very deep local energy minimum, so that reaction would not be able to escape it. This result implies that **IM2** is not an intermediate in the modeled reaction and therefore there should be a different pathway for the formation of product **3b** from **IM1**.

Taking a closer look at **IM1** (Scheme 5), one can notice that the spatial proximity of COO^- and OAc groups make it possible for the former to catalyze nucleophilic addition of a TFE molecule to the latter. We were, indeed, able to locate the corresponding transition state (**TS2**), which turned out to have an easily accessible free energy of 21.8 kcal mol^{-1}. Notably, this energy barrier is considerably lower than the activation energy of the **IM1** → **IM2** transition (estimated to be ≥25.8 kcal

https://doi.org/10.1021/acs.joc.2c01634
J. Org. Chem. 2022, 87, 13980−13989

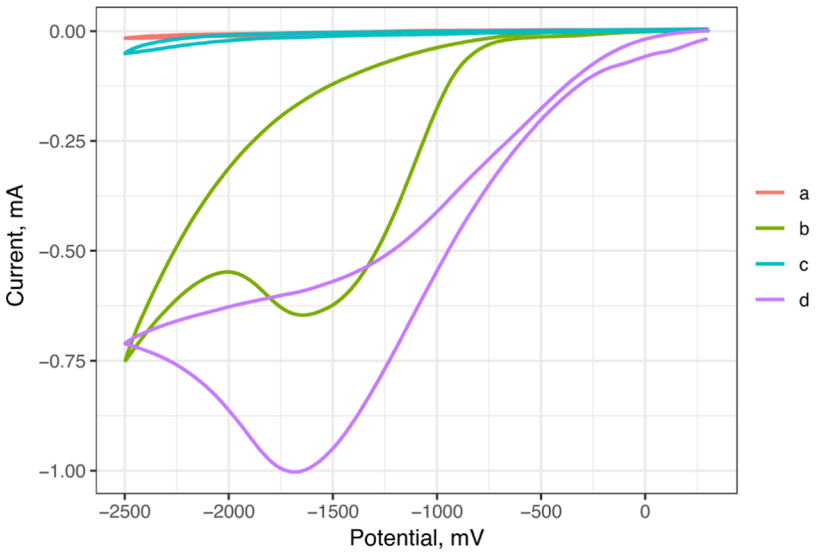

Figure 1. CV curves on a working glassy-carbon electrode (d = 3 mm) *vs* $Ag/AgNO_3$ reference electrode under a scan rate of 0.1 V s^{-1} for 0.1 M *n*-Bu_4NClO_4 solutions: (a) background in CH_3CN (red) and (b) cyclopropyl malonoyl peroxide **2** (0.05 M) in CH_3CN (green) and (c) background in CF_3CH_2OH (blue) and (d) cyclopropyl malonoyl peroxide **2** (0.05 M) in CF_3CH_2OH (purple).

Scheme 4. Nucleophilic Attack Step with Computed Relative Free Energies of Intermediates and Transition States (Cyan) and Reaction Barriers (Pink, in kcal mol^{-1})[a]

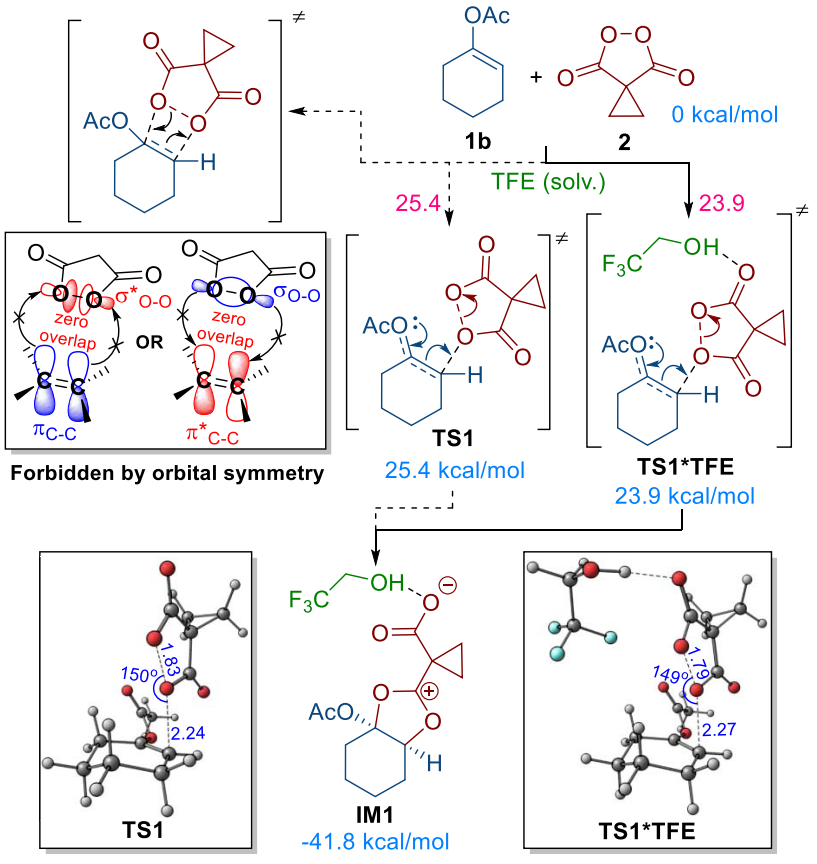

[a]Solid arrows correspond to the main reaction route and the dashed ones denote a hypothetical (2 + 2)-addition mechanism and an unfavorable pathway *via* solvent-unassisted **TS1**.

mol^{-1}, see SI), in complete agreement with our conclusion that **IM2** does not form in the course of the reaction.

Intrigued by the ability of the carboxyl anion to facilitate the attack of TFE at the acyl group, we have tested the possibility of concerted S_N2@O and deacylation processes supposing that the formed COO^- group can simultaneously deprotonate TFE. We hypothesized three such TSs and prepared the starting structures for saddle-point optimizations using preoptimization

https://doi.org/10.1021/acs.joc.2c01634
J. Org. Chem. 2022, 87, 13980−13989

Scheme 5. Elimination of Acetyl Group with Computed Relative Free Energies of Intermediates and Transition States (Cyan) and Reaction Barriers (Pink, in kcal mol^{-1})[a]

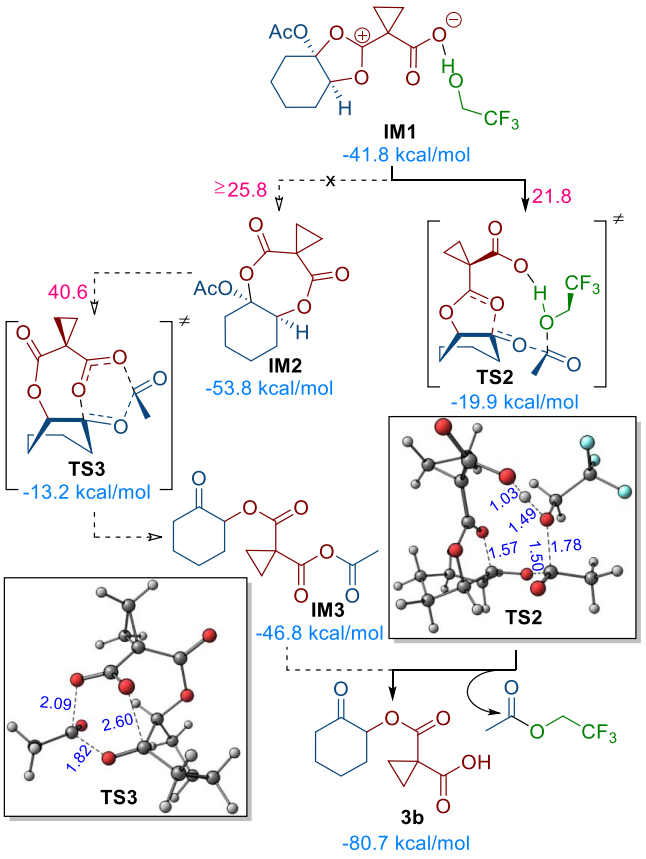

[a]Solid arrows denote the main reaction route and the dashed ones correspond to kinetically unfavorable pathways.

procedure[89] (optimizing their geometries with constraints on the bonds that are expected to form/break *via* these TSs; Figure 3). In all cases, preoptimized geometries possessed an imaginary vibrational mode corresponding to the desired TSs. However, the following saddle-point optimizations failed to converge to TSs of S_N2@O concerted with deacylation (Figure 3). Relaxing the constraint on O−H distance led to identical results (Figure S6). These results indicate that S_N2@O and deacylation proceed in steps.

Thus, the modeling shows that both stages of the reaction demand protic and nucleophilic solvents. In the first stage, solvent effects due to electrostatics and hydrogen bonding lower the S_N2@O activation energy by 3.0 kcal mol^{-1}. The formed **IM1** possesses a highly basic carboxylate group close to the acetyl moiety, enabling intramolecular base catalysis, where the carboxylate group deprotonates a TFE molecule, inducing its nucleophilic attack at the acetyl group. The last step is accompanied by the cleavage of the transiently formed five-membered ring to afford the final product **3b**. The eliminated CF_3CH_2OAc was detected in the reaction mixture (SI, Page S21). Strikingly, this intramolecular catalysis allows the reaction to evade the seven-membered intermediate **IM2**, whose formation was detected experimentally and proved computationally in similar reactions with OMe-substituted vinyl ethers, *i.e.*, the substrates lacking the key acetyl group.[36,37]

CONCLUSIONS

Organic peroxides provide an umpolung approach for the introduction of OR-moiety into organic molecules as an electrophilic "$^{+}$OR" synthon instead the usual nucleophilic "$^{-}$OR" species. We show that the oxidative functionalization of enol acetates with cyclic diacyl peroxides proceeds *via* bimolecular nucleophilic substitution at the oxygen atom of peroxide with subsequent deacylation mediated by trifluoroethanol. This process provides convenient access to α-acyloxyketones, prepared in 28−87% yields. The computational analysis demonstrates the dual role of trifluoroethanol in

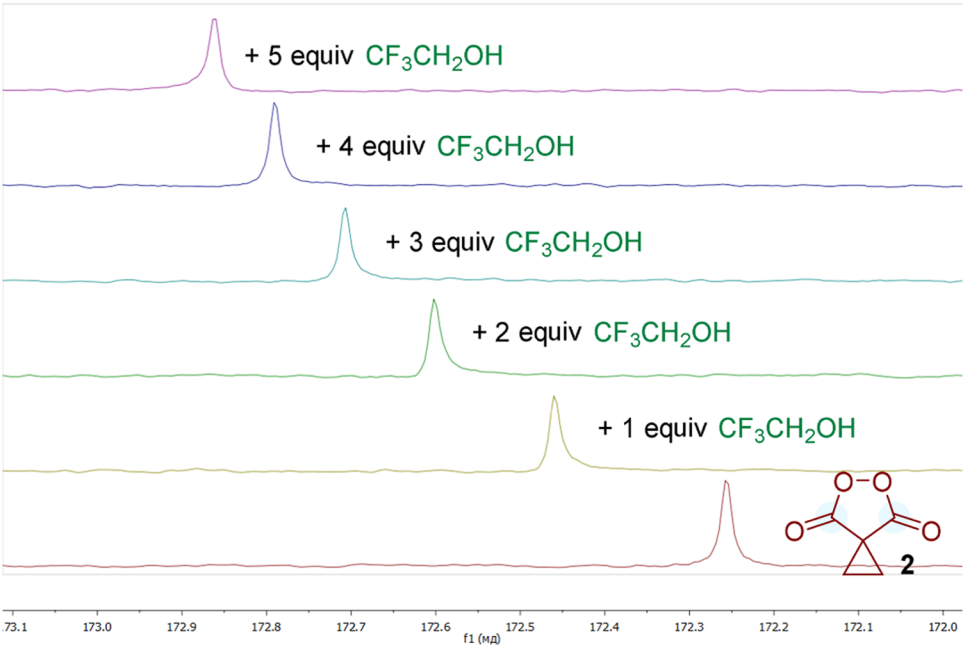

Figure 2. ^{13}C NMR chemical shifts observed in the titration of peroxide **2** with CF_3CH_2OH (solvent $CDCl_3$).

https://doi.org/10.1021/acs.joc.2c01634
J. Org. Chem. 2022, 87, 13980−13989

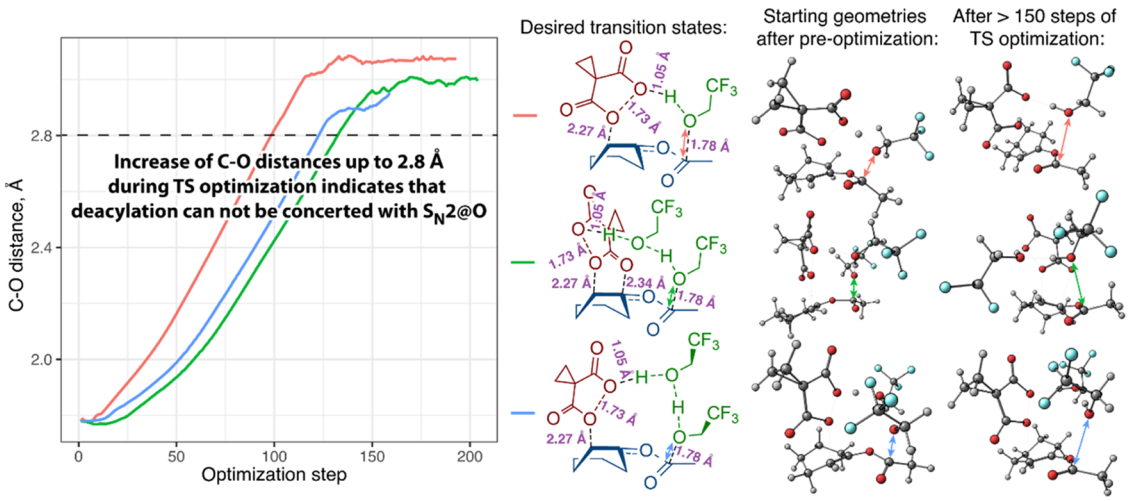

Figure 3. Results of the search for three hypothesized TSs of concerted $S_N2@O$ and deacylation steps. Bond lengths constrained during preoptimization of each TS are given in purple.

stabilizing the transition state of the $S_N2@O$ step and assisting in the acetyl elimination step.

EXPERIMENTAL SECTION

Experimental Procedure for Scheme 3. Cyclic diacyl peroxide **2**, **4**, or **6** (1.1 mmol, 1.1 equiv) was added to a solution of **1** (1.0 mmol, 1.0 equiv) in CF_3CH_2OH (2 mL) at 20−25 °C. The reaction mixture was refluxed (heating mantle) until the complete conversion of **1** was observed by TLC (2−5 h). Later, the reaction mixture was concentrated under reduced pressure using a rotary evaporator (15−20 mmHg) (a water bath temperature, *ca.* 40 °C). Each product (**3**, **5**, and **7**) was isolated by both methods (A and B). The best isolated yield of **3**, **5**, or **7** is given.

Isolation Method A. The reaction mixture was transferred to the top of the chromatographic column and the product (**3e**, **3f**, **3i**, **5k**, **3o**, **3p**) was isolated by column chromatography on SiO_2 (PE/EtOAc = from 8:1 to 2:1).

Isolation Method B. The reaction mixture was concentrated under reduced pressure using a rotary evaporator (15−20 mmHg) (a water bath temperature, *ca.* 40 °C). Then, CH_2Cl_2 (2 mL) and a solution of $NaHCO_3$ (2.5 mmol, 210.0 mg, 2.5 equiv) in H_2O (2 mL) were added to the reaction mixture. The resulting mixture was stirred for 1 h at 20−25 °C. Later, H_2O (50 mL) was added. The mixture was washed with petroleum ether (4 × 5 mL). Later, the aqueous layer was washed with a 0.1 M solution of formic acid in Et_2O (3 × 20 mL). Combined organic layers were dried over $MgSO_4$, filtered, and concentrated under reduced pressure using a rotary evaporator (15−20 mmHg) (a water bath temperature, *ca.* 20−25 °C). The product (**3a−d**, **3g**, **3h**, **3j−l**, **7k**) did not require further purification.

ASSOCIATED CONTENT

Data Availability Statement

The data underlying this study are available in the published article and its online supplementary material.

Supporting Information

The Supporting Information is available free of charge at https://pubs.acs.org/doi/10.1021/acs.joc.2c01634.

Detailed experimental procedures, materials, and methods, ^1H and ^{13}C NMR spectra for all compounds, HRMS data, and computational details (PDF)

Computational data and structures of all calculated molecules and transition states (XYZ)

AUTHOR INFORMATION

Corresponding Authors

Igor V. Alabugin − *Department of Chemistry and Biochemistry, Florida State University, Tallahassee, Florida 32306, United States;* orcid.org/0000-0001-9289-3819; Email: alabugin@chem.fsu.edu

Alexander O. Terent'ev − *N. D. Zelinsky Institute of Organic Chemistry, Russian Academy of Sciences, Moscow 119991, Russian Federation;* orcid.org/0000-0001-8018-031X; Email: terentev@ioc.ac.ru

Authors

Vera A. Vil' − *N. D. Zelinsky Institute of Organic Chemistry, Russian Academy of Sciences, Moscow 119991, Russian Federation;* orcid.org/0000-0002-6847-6035

Evgenii S. Gorlov − *N. D. Zelinsky Institute of Organic Chemistry, Russian Academy of Sciences, Moscow 119991, Russian Federation*

Diana V. Shuingalieva − *N. D. Zelinsky Institute of Organic Chemistry, Russian Academy of Sciences, Moscow 119991, Russian Federation; D. Mendeleev University of Chemical Technology of Russia, Moscow 125047, Russian Federation*

Artem Yu. Kunitsyn − *N. D. Zelinsky Institute of Organic Chemistry, Russian Academy of Sciences, Moscow 119991, Russian Federation*

Nikolai V. Krivoshchapov − *N. D. Zelinsky Institute of Organic Chemistry, Russian Academy of Sciences, Moscow 119991, Russian Federation*

Michael G. Medvedev − *N. D. Zelinsky Institute of Organic Chemistry, Russian Academy of Sciences, Moscow 119991, Russian Federation;* orcid.org/0000-0001-7070-4052

Complete contact information is available at: https://pubs.acs.org/10.1021/acs.joc.2c01634

Notes

The authors declare no competing financial interest.

ACKNOWLEDGMENTS

The synthesis of peroxides and experimental studies of oxidative functionalization were supported by the Russian Science Foundation (Grant No. 21-13-00205, E.S.G. and A.O.T.). Quantum chemical calculations were performed with

financial support from the Ministry of Science and Higher Education of the Russian Federation. The computational analysis at FSU was supported by the U.S. National Science Foundation (CHE-2102579, I.V.A.). The Siberian Branch of the Russian Academy of Sciences (SB RAS) Siberian Supercomputer Center is gratefully acknowledged for providing supercomputer facilities. The research is carried out using the equipment of the shared research facilities of HPC computing resources at Lomonosov Moscow State University.[96] This work has been carried out using computing resources of the federal collective usage center Complex for Simulation and Data Processing for Mega-science Facilities at NRC "Kurchatov Institute", http://ckp.nrcki.ru/. The authors acknowledge the computational resources provided by Moscow State University's Faculty of Computational Mathematics and Cybernetics (IBM Blue Gene/P, Polus).

REFERENCES

(1) Bunnett, J. F.; Zahler, R. E. Aromatic Nucleophilic Substitution Reactions. *Chem. Rev.* **1951**, *49*, 273−412.
(2) Van der Plas, H. C. The SN(ANRORC) mechanism: a new mechanism for nucleophilic substitution. *Acc. Chem. Res.* **1978**, *11*, 462−468.
(3) Kolodiazhnyi, O. I.; Kolodiazhna, A. Nucleophilic substitution at phosphorus: stereochemistry and mechanisms. *Tetrahedron: Asymmetry* **2017**, *28*, 1651−1674.
(4) Tillett, J. G. Nucleophilic substitution at tricoordinate sulfur. *Chem. Rev.* **1976**, *76*, 747−772.
(5) Holmes, R. R. The stereochemistry of nucleophilic substitution of tetracoordinate silicon. *Chem. Rev.* **1990**, *90*, 17−31.
(6) Augustine, R. L. The Reaction of Eneamines with Benzoyl Peroxide1. *J. Org. Chem.* **1963**, *28*, 581−582.
(7) Lawesson, S.-O.; Grönwall, S.; et al. Studies on Peroxy Compounds. VI. A Novel Method for the Preparations of Acyloins. *Acta Chem. Scand.* **1960**, *14*, 1445−1446.
(8) Wang, Y.; Gao, Q.; Liu, Z.; Bai, S.; Tang, X.; Yin, H.; Meng, Q. Enantioselective α-Benzoyloxylation of β-Keto Esters by N-Oxide Phase-Transfer Catalysts. *J. Org. Chem.* **2018**, *83*, 2263−2273.
(9) Wang, Y.; Gao, Q.; Li, N.; Chen, Y.; Cui, J.; Gao, F.; Meng, Q. High-efficiency α-benzoyloxylation and hydroxylation of β-keto amides by phase transfer catalysis. *Tetrahedron* **2018**, *74*, 4126−4133.
(10) Arimitsu, S.; Gima, E. Improvement of primary-amine-catalyzed asymmetric α-benzoyloxylation of α-branched enals by a synergistic effect of water and sulfonic acids. *Tetrahedron Lett.* **2020**, *61*, No. 152032.
(11) Kawamura, S.; Mukherjee, S.; Sodeoka, M. Recent advances in reactions using diacyl peroxides as sources of O- and C-functional groups. *Org. Biomol. Chem.* **2021**, *19*, 2096−2109.
(12) Liu, H.; Yu, J.-T.; Pan, C. Diacyl peroxides: practical reagents as aryl and alkyl radical sources. *Chem. Commun.* **2021**, *57*, 6707−6724.
(13) Lawesson, S.-O.; Yang, N. C. Reactions of Grignard Reagents with Peroxy Compounds1,2. *J. Am. Chem. Soc.* **1959**, *81*, 4230−4233.
(14) Gore, M. P.; Vederas, J. C. Oxidation of enolates by dibenzyl peroxydicarbonate to carbonates of.alpha.-hydroxy carbonyl compounds. *J. Org. Chem.* **1986**, *51*, 3700−3704.
(15) Hoffman, R. V.; Kim, H. O. Synthesis of 2-[[(p-nitrophenyl)-sulfonyl]oxy] esters from ketene silyl acetals and bis[(p-nitrophenyl)-sulfonyl] peroxide. *J. Org. Chem.* **1988**, *53*, 3855−3857.
(16) Hoffman, R. V.; Wilson, A. L.; Kim, H. O. Synthesis of 2-[[(p-nitrophenyl)sulfonyl]oxy] 3-keto esters from 3-keto esters and (p-nitrophenyl)sulfonyl peroxide. *J. Org. Chem.* **1990**, *55*, 1267−1270.
(17) Dannley, R. L.; Corbett, G. E. Nitrobenzenesulfonyl Peroxides as Reagents for Aromatic Substitution1. *J. Org. Chem.* **1966**, *31*, 153−156.
(18) Matsubara, S.; Takai, K.; Nozaki, H. Baeyer-Villiger Oxidation with $Me_3SiOOSiMe_3$ under Assistance of $SnCl_4$ or $BF_3{\cdot}OEt_2$. *Bull. Chem. Soc. Jpn.* **1983**, *56*, 2029−2032.
(19) Davidson, S. C.; dos Passos Gomes, G.; Kuhn, L. R.; Alabugin, I. V.; Kennedy, A. R.; Tomkinson, N. C. O. Organocatalytic sulfoxidation. *Tetrahedron* **2021**, *78*, No. 131784.
(20) Zhao, R.; Chang, D.; Shi, L. Recent Advances in Cyclic Diacyl Peroxides: Reactivity and Selectivity Enhancement Brought by the Cyclic Structure. *Synthesis* **2017**, *49*, 3357−3365.
(21) Greene, F. D. Cyclic Diacyl Peroxides. I. Monomeric Phthaloyl Peroxide1. *J. Am. Chem. Soc.* **1956**, *78*, 2246−2250.
(22) Greene, F. D. Cyclic Diacyl Peroxides. II. Reaction of Phthaloyl Peroxide with cis- and trans-Stilbene. *J. Am. Chem. Soc.* **1956**, *78*, 2250−2254.
(23) Greene, F. D.; Rees, W. W. Cyclic Diacyl Peroxides. III.1 The Reaction of Phthaloyl Peroxide with Olefins. *J. Am. Chem. Soc.* **1958**, *80*, 3432−3437.
(24) Adam, W.; Rucktaeschel, R. Photolysis and thermolysis of di-n-butylmalonyl peroxide. Evidence for.alpha.-lactone intermediates. *J. Org. Chem.* **1978**, *43*, 3886−3890.
(25) Adam, W.; Rucktaeschel, R. Cyclic peroxides. XVII. Solvolysis of dibutylmalonoyl peroxide. *J. Org. Chem.* **1972**, *37*, 4128−4133.
(26) Yuan, C.; Axelrod, A.; Varela, M.; Danysh, L.; Siegel, D. Synthesis and reaction of phthaloyl peroxide derivatives, potential organocatalysts for the stereospecific dihydroxylation of alkenes. *Tetrahedron Lett.* **2011**, *52*, 2540−2542.
(27) Yuan, C.; Liang, Y.; Hernandez, T.; Berriochoa, A.; Houk, K. N.; Siegel, D. Metal-free oxidation of aromatic carbon−hydrogen bonds through a reverse-rebound mechanism. *Nature* **2013**, *499*, 192−196.
(28) Eliasen, A. M.; Christy, M.; Claussen, K. R.; Besandre, R.; Thedford, R. P.; Siegel, D. Dearomatization Reactions Using Phthaloyl Peroxide. *Org. Lett.* **2015**, *17*, 4420−4423.
(29) Camelio, A. M.; Liang, Y.; Eliasen, A. M.; Johnson, T. C.; Yuan, C.; Schuppe, A. W.; Houk, K. N.; Siegel, D. Computational and Experimental Studies of Phthaloyl Peroxide-Mediated Hydroxylation of Arenes Yield a More Reactive Derivative, 4,5-Dichlorophthaloyl Peroxide. *J. Org. Chem.* **2015**, *80*, 8084−8095.
(30) Griffith, J. C.; Jones, K. M.; Picon, S.; Rawling, M. J.; Kariuki, B. M.; Campbell, M.; Tomkinson, N. C. O. Alkene Syn Dihydroxylation with Malonoyl Peroxides. *J. Am. Chem. Soc.* **2010**, *132*, 14409−14411.
(31) Rawling, M. J.; Tomkinson, N. C. O. Metal-free syn-dioxygenation of alkenes. *Org. Biomol. Chem.* **2013**, *11*, 1434−1440.
(32) Jones, K. M.; Tomkinson, N. C. O. Metal-Free Dihydroxylation of Alkenes using Cyclobutane Malonoyl Peroxide. *J. Org. Chem.* **2012**, *77*, 921−928.
(33) Terent'ev, A. O.; Vil', V. A.; Gorlov, E. S.; Rusina, O. N.; Korlyukov, A. A.; Nikishin, G. I.; Adam, W. Selective Oxidative Coupling of 3H-Pyrazol-3-ones, Isoxazol-5(2H)-ones, Pyrazolidine-3,5-diones, and Barbituric Acids with Malonyl Peroxides: An Effective C-O Functionalization. *ChemistrySelect* **2017**, *2*, 3334−3341.
(34) Terent'ev, A. O.; Vil', V. A.; Nikishin, G. I.; Adam, W. Lanthanide-Catalyzed Oxidative C−O Coupling of 1,3-Dicarbonyl Compounds with Diacyl Peroxides. *Synlett* **2015**, *26*, 802−806.
(35) Terent'ev, A. O.; Vil', V. A.; Gorlov, E. S.; Nikishin, G. I.; Pivnitsky, K. K.; Adam, W. Lanthanide-Catalyzed Oxyfunctionalization of 1,3-Diketones, Acetoacetic Esters, And Malonates by Oxidative C−O Coupling with Malonyl Peroxides. *J. Org. Chem.* **2016**, *81*, 810−823.
(36) Vil', V. A.; Gorlov, E. S.; Bityukov, O. V.; Barsegyan, Y. A.; Romanova, Y. E.; Merkulova, V. M.; Terent'ev, A. O. C−O coupling of Malonyl Peroxides with Enol Ethers via [5+2] Cycloaddition: Non-Rubottom Oxidation. *Adv. Synth. Catal.* **2019**, *361*, 3173−3181.
(37) Vil', V. A.; Gorlov, E. S.; Yu, B.; Terent'ev, A. O. Oxidative α-acyloxylation of acetals with cyclic diacyl peroxides. *Org. Chem. Front.* **2021**, *8*, 3091−3101.
(38) Zeng, Y.; Chiou, M.-F.; Zhu, X.; Cao, J.; Lv, D.; Jian, W.; Li, Y.; Zhang, X.; Bao, H. Copper-Catalyzed Enantioselective Radical 1,4-Difunctionalization of 1,3-Enynes. *J. Am. Chem. Soc.* **2020**, *142*, 18014−18021.

https://doi.org/10.1021/acs.joc.2c01634
J. Org. Chem. 2022, 87, 13980−13989

(39) Zeng, Y.; Li, Y.; Lv, D.; Bao, H. Copper-catalyzed three-component oxycyanation of alkenes. *Org. Chem. Front.* **2021**, *8*, 908−914.
(40) Ge, L.; Li, Y.; Jian, W.; Bao, H. Alkyl Esterification of Vinylarenes Enabled by Visible-Light-Induced Decarboxylation. *Chem. - Eur. J.* **2017**, *23*, 11767−11770.
(41) Alabugin, I. V.; Kuhn, L.; Medvedev, M. G.; Krivoshchapov, N. V.; Vil', V. A.; Yaremenko, I. A.; Mehaffy, P.; Yarie, M.; Terent'ev, A. O.; Zolfigol, M. A. Stereoelectronic power of oxygen in control of chemical reactivity: the anomeric effect is not alone. *Chem. Soc. Rev.* **2021**, *50*, 10253−10345.
(42) Kyasa, S.; Meier, R. N.; Pardini, R. A.; Truttmann, T. K.; Kuwata, K. T.; Dussault, P. H. Synthesis of Ethers via Reaction of Carbanions and Monoperoxyacetals. *J. Org. Chem.* **2015**, *80*, 12100−12114.
(43) Vedejs, E.; Engler, D. A.; Telschow, J. E. Transition-metal peroxide reactions. Synthesis of.alpha.-hydroxycarbonyl compounds from enolates. *J. Org. Chem.* **1978**, *43*, 188−196.
(44) Vedejs, E. Method for direct hydroxylation of enolates. Transition metal peroxide reactions. *J. Am. Chem. Soc.* **1974**, *96*, 5944−5946.
(45) Anderson, J. C.; Smith, S. C. Oxodiperoxymolybdenum-(pyridine)-1,3-dimethyl-3,4,5,6-tetrahydro-2(1H)-pyrimidinone (MoO5.Py.DMPU): A Safer Alternative to MoOPH for the α-Hydroxylation of Carbonyl Compounds. *Synlett* **1990**, *1990*, 107−108.
(46) Davis, F. A.; Haque, M. S. Stereochemistry of the asymmetric oxidation of ketone enolates using (camphorylsulfonyl)oxaziridines. *J. Org. Chem.* **1986**, *51*, 4083−4085.
(47) Davis, F. A.; Weismiller, M. C. Enantioselective synthesis of tertiary.alpha.-hydroxy carbonyl compounds using [(8,8-dichlorocamphoryl)sulfonyl]oxaziridine. *J. Org. Chem.* **1990**, *55*, 3715−3717.
(48) Williamson, K. S.; Michaelis, D. J.; Yoon, T. P. Advances in the Chemistry of Oxaziridines. *Chem. Rev.* **2014**, *114*, 8016−8036.
(49) Zou, L.; Wang, B.; Mu, H.; Zhang, H.; Song, Y.; Qu, J. Development of Tartaric Acid Derived Chiral Guanidines and Their Application to Catalytic Enantioselective α-Hydroxylation of β-Dicarbonyl Compounds. *Org. Lett.* **2013**, *15*, 3106−3109.
(50) Ishimaru, T.; Shibata, N.; Nagai, J.; Nakamura, S.; Toru, T.; Kanemasa, S. Lewis Acid-Catalyzed Enantioselective Hydroxylation Reactions of Oxindoles and β-Keto Esters Using DBFOX Ligand. *J. Am. Chem. Soc.* **2006**, *128*, 16488−16489.
(51) Toullec, P. Y.; Bonaccorsi, C.; Mezzetti, A.; Togni, A. Expanding the scope of asymmetric electrophilic atom-transfer reactions: Titanium- and ruthenium-catalyzed hydroxylation of β-ketoesters. *Proc. Natl. Acad. Sci. U.S.A.* **2004**, *101*, 5810−5814.
(52) Davis, F. A.; Sheppard, A. C.; Chen, B. C.; Haque, M. S. Chemistry of oxaziridines. 14. Asymmetric oxidation of ketone enolates using enantiomerically pure (camphorylsulfonyl)oxaziridine. *J. Am. Chem. Soc.* **1990**, *112*, 6679−6690.
(53) Takechi, S.; Kumagai, N.; Shibasaki, M. Catalytic asymmetric hydroxylation of α-alkoxycarbonyl amides with a $Pr(OiPr)_3$/amide-based ligand catalyst. *Tetrahedron Lett.* **2011**, *52*, 2140−2143.
(54) Lin, X.; Ruan, S.; Yao, Q.; Yin, C.; Lin, L.; Feng, X.; Liu, X. Kinetic Resolution of Oxaziridines via Chiral Bifunctional Guanidine-Catalyzed Enantioselective α-Hydroxylation of β-Keto Esters. *Org. Lett.* **2016**, *18*, 3602−3605.
(55) Davis, F. A.; Chen, B. C. Asymmetric hydroxylation of enolates with N-sulfonyloxaziridines. *Chem. Rev.* **1992**, *92*, 919−934.
(56) Davis, F. A.; Towson, J. C.; Weismiller, M. C.; Lal, S.; Carroll, P. J. Chemistry of oxaziridines. 11. (Camphorylsulfonyl)oxaziridine: synthesis and properties. *J. Am. Chem. Soc.* **1988**, *110*, 8477−8482.
(57) Picon, S.; Rawling, M.; Campbell, M.; Tomkinson, N. C. O. Alkene Dihydroxylation with Malonoyl Peroxides: Catalysis Using Fluorinated Alcohols. *Org. Lett.* **2012**, *14*, 6250−6253.
(58) Dragan, A.; Kubczyk, T. M.; Rowley, J. H.; Sproules, S.; Tomkinson, N. C. O. Arene Oxidation with Malonoyl Peroxides. *Org. Lett.* **2015**, *17*, 2618−2621.
(59) Alamillo-Ferrer, C.; Karabourniotis-Sotti, M.; Kennedy, A. R.; Campbell, M.; Tomkinson, N. C. O. Alkene Dioxygenation with Malonoyl Peroxides: Synthesis of γ-Lactones, Isobenzofuranones, and Tetrahydrofurans. *Org. Lett.* **2016**, *18*, 3102−3105.
(60) Alamillo-Ferrer, C.; Curle, J. M.; Davidson, S. C.; Lucas, S. C. C.; Atkinson, S. J.; Campbell, M.; Kennedy, A. R.; Tomkinson, N. C. O. Alkene Oxyamination Using Malonoyl Peroxides: Preparation of Pyrrolidines and Isoxazolidines. *J. Org. Chem.* **2018**, *83*, 6728−6740.
(61) Wencel-Delord, J.; Colobert, F. A remarkable solvent effect of fluorinated alcohols on transition metal catalysed C-H functionalizations. *Org. Chem. Front.* **2016**, *3*, 394−400.
(62) Shuklov, I. A.; Dubrovina, N. V.; Börner, A. Fluorinated Alcohols as Solvents, Cosolvents and Additives in Homogeneous Catalysis. *Synthesis* **2007**, *2007*, 2925−2943.
(63) Sohail, M.; Zhang, Y.; Sun, G.; Guo, X.; Liu, W.; Liu, C.; Zhao, Z. K. Four-component reaction leading to highly functionalized sulfoalkoxy carbonyl compounds. *Chem. Commun.* **2015**, *51*, 4774−4777.
(64) Sohail, M.; Khan, M.; Zhang, Y.; Peng, C.; Chen, Q.; Zhao, Z. K. Four-component electrophilic difunctionalization of olefins using sulfonic acids, cyclic ethers, and NBS. *Tetrahedron Lett.* **2015**, *56*, 5743−5746.
(65) Deruer, E.; Hamel, V.; Blais, S.; Canesi, S. Rapid transformation of sulfinate salts into sulfonates promoted by a hypervalent iodine(III) reagent. *Beilstein J. Org. Chem.* **2018**, *14*, 1203−1207.
(66) Donkers, R. L.; Workentin, M. S. First Determination of the Standard Potential for the Dissociative Reduction of the Antimalarial Agent Artemisinin. *J. Phys. Chem. B* **1998**, *102*, 4061−4063.
(67) Donkers, R. L.; Maran, F.; Wayner, D. D. M.; Workentin, M. S. Kinetics of the Reduction of Dialkyl Peroxides. New Insights into the Dynamics of Dissociative Electron Transfer1. *J. Am. Chem. Soc.* **1999**, *121*, 7239−7248.
(68) Donkers, R. L.; Workentin, M. S. Kinetics of Dissociative Electron Transfer to Ascaridole and Dihydroascaridole—Model Bicyclic Endoperoxides of Biological Relevance. *Chem. - Eur. J.* **2001**, *7*, 4012−4020.
(69) Donkers, R. L.; Workentin, M. S. Elucidation of the Electron Transfer Reduction Mechanism of Anthracene Endoperoxides. *J. Am. Chem. Soc.* **2004**, *126*, 1688−1698.
(70) Stringle, D. L. B.; Magri, D. C.; Workentin, M. S. Efficient Homogeneous Radical-Anion Chain Reactions Initiated by Dissociative Electron Transfer to 3,3,6,6-Tetraaryl-1,2-dioxanes. *Chem. - Eur. J.* **2010**, *16*, 178−188.
(71) dos Passos Gomes, G.; Wimmer, A.; Smith, J. M.; Konig, B.; Alabugin, I. V. CO_2 or SO_2: Should It Stay, or Should It Go? *J. Org. Chem.* **2019**, *84*, 6232−6243.
(72) Kuhn, L.; Vil', V. A.; Barsegyan, Y. A.; Terent'ev, A. O.; Alabugin, I. V. Carboxylate as a Non-innocent L-Ligand: Computational and Experimental Search for Metal-Bound Carboxylate Radicals. *Org. Lett.* **2022**, *24*, 3817−3822.
(73) Magri, D. C.; Workentin, M. S. A Radical-Anion Chain Mechanism Initiated by Dissociative Electron Transfer to a Bicyclic Endoperoxide: Insight into the Fragmentation Chemistry of Neutral Biradicals and Distonic Radical Anions. *Chem. - Eur. J.* **2008**, *14*, 1698−1709.
(74) Rawling, M. J.; Rowley, J. H.; Campbell, M.; Kennedy, A. R.; Parkinson, J. A.; Tomkinson, N. C. O. Mechanistic insights into the malonoyl peroxide syn-dihydroxylation of alkenes. *Chem. Sci.* **2014**, *5*, 1777−1785.
(75) Adamo, C.; Barone, V. Toward reliable density functional methods without adjustable parameters: The PBE0 model. *J. Chem. Phys.* **1999**, *110*, 6158−6170.
(76) Grimme, S.; Antony, J.; Ehrlich, S.; Krieg, H. A consistent and accurate ab initio parametrization of density functional dispersion correction (DFT-D) for the 94 elements H-Pu. *J. Chem. Phys.* **2010**, *132*, No. 154104.
(77) Spitznagel, G. W.; Clark, T.; von Ragué Schleyer, P.; Hehre, W. J. An evaluation of the performance of diffuse function-augmented

https://doi.org/10.1021/acs.joc.2c01634
J. Org. Chem. 2022, 87, 13980−13989

basis sets for second row elements, Na-Cl. *J. Comput. Chem.* **1987**, *8*, 1109−1116.
(78) Clark, T.; Chandrasekhar, J.; Spitznagel, G. W.; Schleyer, P. V. R. Efficient diffuse function-augmented basis sets for anion calculations. III. The 3-21+G basis set for first-row elements, Li−F. *J. Comput. Chem.* **1983**, *4*, 294−301.
(79) Francl, M. M.; Pietro, W. J.; Hehre, W. J.; Binkley, J. S.; Gordon, M. S.; DeFrees, D. J.; Pople, J. A. Self-consistent molecular orbital methods. XXIII. A polarization-type basis set for second-row elements. *J. Chem. Phys.* **1982**, *77*, 3654−3665.
(80) McLean, A. D.; Chandler, G. S. Contracted Gaussian basis sets for molecular calculations. I. Second row atoms, Z=11−18. *J. Chem. Phys.* **1980**, *72*, 5639−5648.
(81) Krishnan, R.; Binkley, J. S.; Seeger, R.; Pople, J. A. Self-consistent molecular orbital methods. XX. A basis set for correlated wave functions. *J. Chem. Phys.* **1980**, *72*, 650−654.
(82) Mennucci, B. Polarizable continuum model. *Wiley Interdiscip. Rev.: Comput. Mol. Sci.* **2012**, *2*, 386−404.
(83) Medvedev, M. G.; Bushmarinov, I. S.; Sun, J.; Perdew, J. P.; Lyssenko, K. A. Density functional theory is straying from the path toward the exact functional. *Science* **2017**, *355*, 49−52.
(84) Marjewski, A. A.; Medvedev, M. G.; Gerasimov, I. S.; Panova, M. V.; Perdew, J. P.; Lyssenko, K. A.; Dmitrienko, A. O. Interplay between test sets and statistical procedures in ranking DFT methods: The case of electron density studies. *Mendeleev Commun.* **2018**, *28*, 225−235.
(85) Mardirossian, N.; Head-Gordon, M. Thirty years of density functional theory in computational chemistry: an overview and extensive assessment of 200 density functionals. *Mol. Phys.* **2017**, *115*, 2315−2372.
(86) Grimme, S. Supramolecular Binding Thermodynamics by Dispersion-Corrected Density Functional Theory. *Chem. - Eur. J.* **2012**, *18*, 9955−9964.
(87) Open-source Python toolkit for processing the results of quantum chemical calculations was used: Luchini, G.; Alegre-Requena, J. V.; Guan, Y.; Funes-Ardoiz, I.; Paton, R. S.GoodVibes, 2019. https://goodvibespy.readthedocs.io/en/latest/#.
(88) Pracht, P.; Bohle, F.; Grimme, S. Automated exploration of the low-energy chemical space with fast quantum chemical methods. *Phys. Chem. Chem. Phys.* **2020**, *22*, 7169−7192.
(89) Medvedev, M. G.; Panova, M. V.; Chilov, G. G.; Bushmarinov, I. S.; Novikov, F. N.; Stroganov, O. V.; Zeifman, A. A.; Svitanko, I. V. Exhaustive conformational search for transition states: the case of catechol O-methyltransferase active site. *Mendeleev Commun.* **2017**, *27*, 224−227.
(90) Yamamoto, H. New reaction and new catalyst—a personal perspective. *Tetrahedron* **2007**, *63*, 8377−8412.
(91) Tanaka, Y.; Xiao, Y. F.; Matsuo, S. Relative permittivity of fluoroalcohols at temperatures from 293 to 323 K and pressures up to 50 MPa. *Fluid Phase Equilib.* **2000**, *170*, 139−149.
(92) Côté, J.-F.; Brouillette, D.; Desnoyers, J. E.; Rouleau, J.-F.; St-Arnaud, J.-M.; Perron, G. Dielectric constants of acetonitrile, γ-butyrolactone, propylene carbonate, and 1,2-dimethoxyethane as a function of pressure and temperature. *J. Solution Chem.* **1996**, *25*, 1163−1173.
(93) Alabugin, I. V. *Stereoelectronic Effects: A Bridge Between Structure and Reactivity*; John Wiley & Sons, Ltd., 2016; pp 284−316.
(94) Simón, L.; Goodman, J. M. Hydrogen-bond stabilization in oxyanion holes: grand jeté to three dimensions. *Org. Biomol. Chem.* **2012**, *10*, 1905−1913.
(95) Coulembier, O.; Sanders, D. P.; Nelson, A.; Hollenbeck, A. N.; Horn, H. W.; Rice, J. E.; Fujiwara, M.; Dubois, P.; Hedrick, J. L. Hydrogen-Bonding Catalysts Based on Fluorinated Alcohol Derivatives for Living Polymerization. *Angew. Chem., Int. Ed.* **2009**, *48*, 5170−5173.
(96) Sadovnichy, V.; Tikhonravov, A.; Voevodin, V.; Opanasenko, V. "Lomonosov": Supercomputing at Moscow State University. In *Contemporary High Performance Computing: From Petascale toward Exascale, Chapman & Hall/CRC Computational Science*; CRC Press: Boca Raton, USA, 2013; pp 283−307.

https://doi.org/10.1021/acs.joc.2c01634
J. Org. Chem. 2022, 87, 13980−13989